

Deletion of a Conserved Noncoding Sequence in *Plzf* Intron Leads to *Plzf* Down-regulation in Limb Bud and Polydactyly in the Rat

František Liška,^{1*} Pavel Šnajdr,^{2†} Lucie Šedová,¹ Ondřej Šeda,¹ Blanka Chylíková,¹ Petra Slámová,¹ Eliška Krejčí,¹ David Sedmera,^{2–4} Miloš Grim,² Drahomíra Křenová,¹ and Vladimír Křen^{1,4}

Lx mutation in SHR.*Lx* rat manifests in homozygotes as hindlimb preaxial polydactyly. It was previously mapped to a chromosome 8 segment containing the *Plzf* gene. *Plzf* (promyelocytic leukemia zinc finger protein) influences limb development as a direct repressor of posterior *HoxD* genes. However, the *Plzf* coding sequence is intact in the *Lx* mutants. Using linkage mapping in F2 hybrids, we downsized the segment containing *Lx* to 155 kb and sequenced conserved noncoding elements (CNEs) inside. A 2,964-bp deletion in *Plzf* intron 2, never detected in control animals, is the only candidate for *Lx*. The deletion removes the most deeply conserved CNE in the 155-kb segment, suggesting a regulatory influence on *Plzf* expression. Correspondingly, using in situ hybridization and quantitative real-time polymerase chain reaction, we found a decrease of *Plzf* expression in *Lx/Lx* limb buds with concomitant anterior expansion of expression domains of its targets, *Hoxd10–13* genes, in the absence of ectopic Sonic hedgehog expression. Upstream regulation of *Plzf* in limb buds is currently unknown. We present here the first candidate *Plzf* cis-regulatory sequence. *Developmental Dynamics* 238: 673–684, 2009. © 2009 Wiley-Liss, Inc.

Key words: promyelocytic leukemia zinc finger (*Plzf*); *HoxD* genes; conserved noncoding element; polydactyly

Accepted 8 December 2008

INTRODUCTION

The tetrapod limb consists of three parts: the proximal stylopod, intermediate zeugopod, and distal autopod. Limb patterning is established along

three axes: proximal to distal (P–D), dorsal to ventral (D–V), and anterior to posterior (A–P), each of them controlled by distinct molecular pathways (Niswander, 2003).

Pentadactyly is the classic digit for-

mula in tetrapods (Galis et al., 2001). An alteration in the number of digits (oligodactyly, polydactyly) is a result of abnormal control of autopod A–P patterning. It is a relatively frequent phenomenon, and in humans, it is con-

ABBREVIATIONS *Bmp* bone morphogenetic protein **BN** Brown Norway rat **bp** base pairs **cM** centimorgan **CNE** conserved noncoding element **CNS** central nervous system **dpc** days post coitum *lu luxoid* (in the mouse) *Lx Luxate* (in the Norway rat) **PD** polydactylous rat **Plzf** promyelocytic leukemia zinc finger **RefSeq** reference sequence database at National Center for Biotechnology Information **SD** Sprague-Dawley rat **Shh** sonic hedgehog **SHR** spontaneously hypertensive rat **SNP** single nucleotide polymorphism **UTR** untranslated region **ZPA** zone of polarizing activity

Additional Supporting Information may be found in the online version of this article.

¹Institute of Biology and Medical Genetics of the 1st Faculty of Medicine and General Teaching Hospital, Charles University in Prague, Praha, Czech Republic

²Institute of Anatomy, 1st Faculty of Medicine, Charles University in Prague, Unemocnice 3, Praha, Czech Republic

³Institute of Animal Physiology and Genetics, Academy of Sciences of the Czech Republic, Praha, Czech Republic

⁴Institute of Physiology, Academy of Sciences of the Czech Republic, Praha, Czech Republic

Grant sponsor: Czech Science Foundation; Grant number: 304/06/0116; Grant number: 301/07/P178; Grant sponsor: European Commission; Grant number: EURATools (LSHG-CT-2005-019015); Grant sponsor: Ministry of Education, Youth and Sports of the Czech Republic; Grant number: MFM 0021620806; Grant sponsor: Academy of Sciences of the Czech Republic; Grant number: AVOZ 50450515.

[†]Drs. Liška and Šnajdr contributed equally to this work.

*Correspondence to: František Liška, Institute of Biology and Medical Genetics of the 1st Faculty of Medicine and General Teaching Hospital, Charles University in Prague, Albertov 4, 128 00 Praha 2, Czech Republic.
E-mail: frantisek.liska@lf1.cuni.cz

DOI 10.1002/dvdy.21859

Published online 3 February 2008 in Wiley InterScience (www.interscience.wiley.com).

sidered to be the most common congenital limb anomaly (Graham and Ress, 1998).

Polydactyly can be classified according to the position of the supernumerary digits as preaxial or postaxial. Preaxial polydactyly, where the supernumerary digits arise at the anterior margin of the autopod, can be further subdivided according to its dependence on ectopic expression of *Sonic hedgehog* (*Shh*). *Shh* expression is confined to the posterior margin of developing limb, in an organizing center called the zone of polarizing activity (ZPA; Riddle et al., 1993). Type 1 polydactyly is dependent on anterior ectopic activation of *Shh* similar to polydactyly induced by anterior transplantation of *Shh*-producing ZPA cells (Yang et al., 1997). Type 2 polydactyly is *Shh*-independent (Talamillo et al., 2005). In both types, the molecular pathway operating during the pathogenesis involves *Hox* genes (Kuijper et al., 2005; Sheth et al., 2007).

Hox genes encode transcription factors and precise activation of their transcription in time and space according to their genomic topography is required for correct definition of the body and limb plan. For limb development, two clusters—*HoxA* and *HoxD*—are essential (Tarchini and Duboule, 2006). *HoxD* genes display asymmetric expression along the A–P axis, indicating their role in control of A–P polarity. Within the *HoxD* cluster, genes belonging to paralogy groups 10 to 13 (*Hoxd10–13*) are the most important for limb development. Generally, *HoxD* genes are activated in two consecutive waves under different transcriptional control (Tarchini and Duboule, 2006; Tarchini et al., 2006). The first phase is essential for development of stylopod and zeugopod. *Hoxd10–13* are expressed in posterodistal nested domains progressively restricted to successively more posterior part of the limb; hence, *Hoxd13* occupies the smallest expression domain located posteriorly. The second phase is essential for autopod development. *Hoxd10–13* are expressed in a presumptive digit domain in a rather reverse pattern compared with the first phase; hence, *Hoxd13* is expressed in the broadest domain. Under physiological situations, *Hoxd10–13* ex-

pression does not extend to the most anterior margin of the limb bud.

Disruption of *Plzf* (promyelocytic leukemia zinc finger, also known as *Zbtb16* or *Zfp145*) function in the mouse by gene targeting leads to multiple patterning defects, including homeotic transformation of axial and limb skeleton and preaxial polydactyly (Barna et al., 2000). In addition, the males are infertile, due to deficiency of spermatogenic stem cell renewal (Buaas et al., 2004; Costoya et al., 2004). Of interest, a recent study revealed that a classic murine mutation *luxoid* (*lu*) is caused by a nonsense point mutation in *Plzf* (Buaas et al., 2004). Recently, loss of *Plzf* function was found in a clinical case. The patient had an 8 Mb deletion of paternal 11q23, including *Plzf* and a point mutation of *Plzf* on the maternal chromosome. In addition to symptoms associated with 11q23 microdeletion syndromes, the patient also presented with absence of thumbs, hypoplasia of radii and ulnae, additional vertebrae and ribs, retarded bone age, and genital hypoplasia. These traits can be ascribed to the loss of *Plzf* function (Fischer et al., 2008).

In addition to limb development and spermatogenesis, *Plzf* has been also implicated in apoptosis (Parrado et al., 2004), cell cycle regulation (Yeyati et al., 1999), tumorigenesis (Piazza et al., 2001; Felicetti et al., 2004), and hematopoiesis (Piazza et al., 2004; Labbaye et al., 2008). Its functional versatility has also been shown by identification of *Plzf* as a crucial member of distinct metabolic and signaling pathways controlling blood pressure (Scheffe et al., 2006; Naray-Fejes-Toth et al., 2008), and angiotensin II-induced cardiac hypertrophy (Senbonmatsu et al., 2003).

Plzf acts as a transcriptional repressor, binding DNA by its C-terminal zinc finger domain containing nine Krüppel type zinc finger motifs (Li et al., 1997; Sitterlin et al., 1997), and recruiting, by its N-terminal bric-a-brac, tramtrack, brad complex/poxvirus zinc finger (BTB/POZ) domain (Bardwell and Treisman, 1994; Dong et al., 1996), transcriptional corepressor complexes with histone deacetylase activity (Hong et al., 1997; David et al., 1998; He et al., 1998). *Plzf* also interacts through its three N-terminal

zinc-finger motifs with nuclear receptors, in particular with retinoic acid receptor (RAR) alpha, blocking the RAR-RXR heterodimerization necessary for retinoic acid signaling (Martin et al., 2003). During limb development, *Plzf* modulates spatial expression of *Hoxd10–13* by transcriptional repression in the anterior part of the developing autopod. The repression mechanism includes direct binding at consensus sequences inside the *HoxD* cluster and recruiting repressor polycomb proteins (Barna et al., 2002). The regulation of *Plzf* expression itself during limb development (i.e., the factor[s] upstream of *Plzf*) is not known.

Mutant allele *Lx* in the rat was described in the 1970s in an outbred rat strain of Wistar origin (Kren, 1975). The mutant rat served as a founder of an inbred strain PD/Cub (polydactylous, PD hereafter). *Lx* was then transferred to genetic backgrounds of BN/Cub (Brown Norway, BN hereafter) and SHR/OlaIpcv (spontaneously hypertensive rat, SHR hereafter) strains, creating thus BN.*Lx* and SHR.*Lx*.PD5 (PD5 hereafter) congenic strains, respectively. The genetic background has significant impact on both expressivity and penetrance of the mutant *Lx* allele: in BN.*Lx* it behaves as semidominant and afflicts also forelimbs. In SHR, *Lx* effects are strictly recessive and restricted to hindlimb autopod (Kren, 1975; Kren et al., 1996). *Lx* is localized to rat chromosome 8 (Kren et al., 1995).

The model for our study is congenic strain PD5. PD5 homozygotes (*Lx/Lx*) display preaxial polydactyly of hindlimbs with 6 triphalangeal toes (plus a digit rudiment between digit I and II), accompanied by a slight alteration in the shape of tarsal bones (Fig. 1). Zeugopod and stylopod are normally formed. Forelimb is not affected. Axial skeleton is never affected. PD5xSHR heterozygotes (+/*Lx*) are indistinguishable from wild-type (+/+). PD5 differential segment contains 14 genes, including *Plzf* (Šeda et al., 2005). Because the autopod malformation resembles the phenotype observed in mouse mutant *lu* (*Plzf^{lu/lu}*) or *Plzf^{-/-}*, *Plzf* is an obvious candidate for the *Lx* phenotype. However, there is an absence of zeugopod, stylopod, and axial skeleton affliction and no signs of male infertility in *Lx/Lx* compared with

both *Plzf*^{-/-} and *Plzf*^{lu/lu}. We showed recently that the *Plzf* coding sequence does not contain any sequence variant specific to rats carrying *Lx* (Šeda et al., 2005). These facts led us to hypothesize that *Lx* is a regulatory mutation in *Plzf*. Because the rat is not used in developmental biology as often as the mouse, we present here a side by side comparison of the limb bud development in the two species (Fig. 2). In general, the rat limb development is approximately 1–2 days delayed, proportional to its 1–2 days longer gestational period.

In this study, we show that *Plzf* expression is markedly reduced in the limb bud of *Lx/Lx* homozygotes. Correspondingly, we found anteriorization of target posterior *HoxD* gene expression. Using intercross, we narrowed the chromosomal segment carrying *Lx* to 155 kb, containing serotonin receptor 5-HT₃ subunit genes *Htr3a*, *Htr3b* (partial), and *Plzf* gene (partial). Surveying all conserved noncoding sequences in the region, we demonstrate that *Lx* homozygotes contain a 2,964-bp deletion that removes the most conserved noncoding element in the 155-kb nonrecombinant region. We conclude that this deletion is likely the cause of the mutant *Lx* phenotype.

RESULTS

Fine Mapping of *Lx* to a 177-kb Segment

In the PD5 congenic strain, *Lx* is contained in a 1.4-Mbp differential segment of PD origin. Because the *Plzf* coding sequence is intact in PD5, we hypothesized that the observed mutant phenotype may be a consequence of a regulatory mutation. The regulatory regions are in general less well defined compared with coding regions. In addition, they can reside anywhere in the differential segment, making it more difficult to compare comprehensively the DNA sequences. Therefore, we decided to downsize the segment carrying *Lx* using F2 hybrids between PD5 and BN. By analysis of 247 F2 hybrids, we found 7 recombinants inside the PD5 differential segment. Two key recombinants refined the *Lx* position to 177 kb (Fig. 3). This region contains 3 genes: *Plzf* (partial), and genes coding subunits of serotonin re-

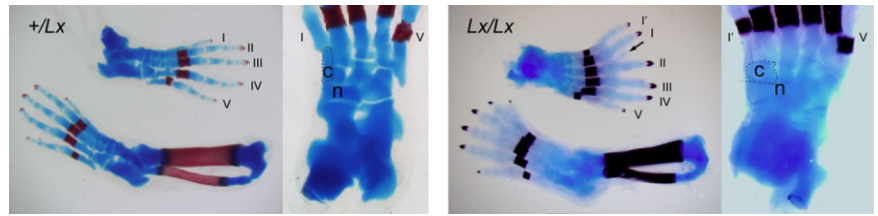


Fig. 1. Limb phenotype of *Lx/Lx* rats compared with *+/Lx* animals. Hind limb sample was taken at 22 days post coitum (dpc; 1 day before birth), bone is stained with Alizarin Red, cartilage with Alcian Blue. *+/Lx* rats show pentadactyly with diphalangeal hallux (wild-type phenotype), *Lx/Lx* rats possess six toes; the extra hallux (I') is triphalangeal. There is an extra skeletal element (rudimentary digit) between the first and second toe (arrow). Tarsal skeletal elements of *Lx/Lx* rats are normal in number, but the anterior elements show alterations in size and shape. In particular the medial cuneiform (labeled "c") lost its elongated shape and widened to accommodate the extra finger ray, accompanied by similar widening of the communicating navicular bone (labeled "n"). Zeugopods are comparable in *Lx/Lx* and *+/Lx* animals and do not differ from *+/+* animals (data not shown; for detailed morphometric analysis of zeugopods, see Printz et al., 2003).

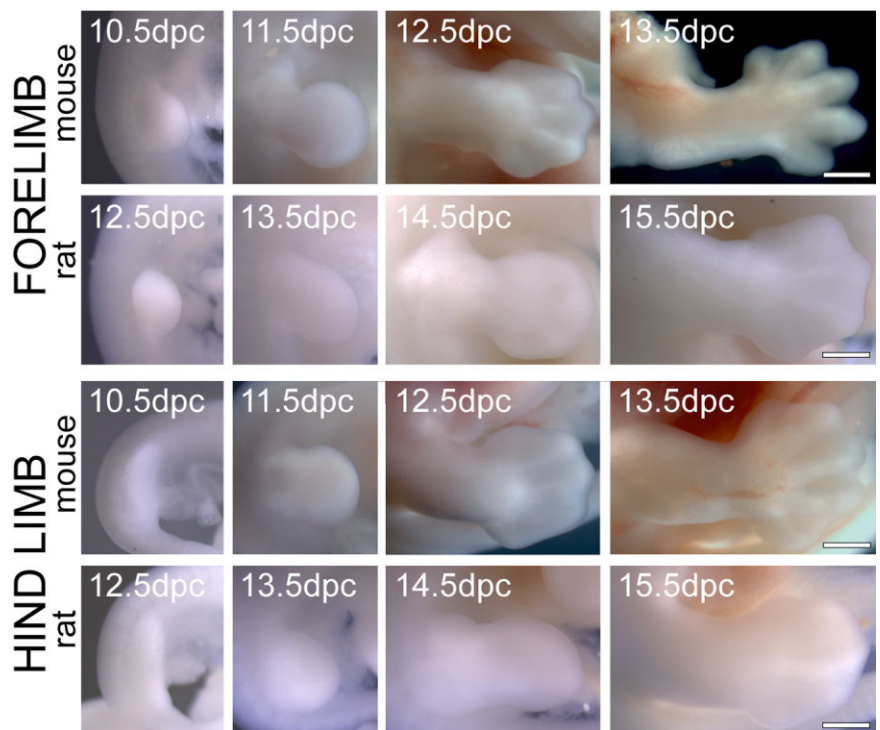


Fig. 2. Gross comparison of mouse (C57BL/6) and rat (SHR) early limb development. Limb buds emerge 2 days later in the rat than they do in the mouse (rat 12.5 days post coitum [dpc] = mouse 10.5 dpc). At 9.5 dpc in the mouse and 11.5 dpc in the rat, we observed similar mesenchymal thickenings in the limb field in both species (data not shown). Interestingly, at the end of our observation period the difference appears closer to 3 days (rat 15.5 dpc = mouse 12.5 dpc). Scale bars = 1 mm.

ceptor 5-HT₃—*Htr3a* and *Htr3b* (partial) (Fig. 4A).

Sequencing Candidate Genes

We sequenced genomic DNA from two strains carrying *Lx* (PD and PD5), and two controls SHR and BN. BN/Cub is a very close relative to BN/SsnHsd, the source of the reference rat genome. Sequence of BN/

Cub determined during this study is identical to the reference genome. Also, sequence of PD and PD5 is identical, as expected, because we assessed only DNA inside the differential segment of PD origin in PD5. When we found a difference between PD and any of the two controls, we expanded our analysis and compared the variant to 9 additional rat strains, including another congenic

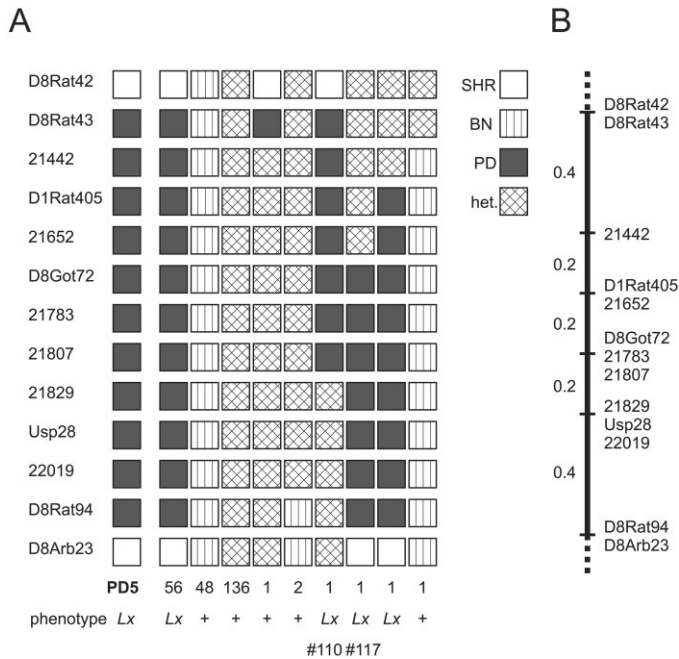


Fig. 3. Fine linkage mapping shows *Lx* is placed between microsatellites 21652 and 21829 (refer to Supp. Table S2 for polymerase chain reaction primers). **A:** Genotypes in F2 (PD5 × BN) hybrids, $n = 247$. The parental congenic strain PD5 (first column) carries *Lx* in its differential segment (of PD origin, dark), flanked by DNA of SHR origin (white). Microsatellite markers follow Mendelian rules (expected ratio PD5:heterozygotes:BN 1:2:1, D8Got72 $\chi^2 = 4.46$; $P = 0.11$), *Lx* segregation is compatible with autosomal recessive mode of inheritance (normal “+”:*Lx* 3:1, $\chi^2 = 0.16$; $P = 0.69$). Two recombinants, No. 110 and 117 are decisive for *Lx* placement between 21652 and 21829. **B:** Linkage map derived from data presented in A. *Lx* segment is 0.4 cM long.

strain carrying *Lx* (BN.*Lx*), paying special attention to strains of Wistar origin (see the Experimental Procedures). Thus, we were able to exclude a role in limb development for every variant shared between *Lx* carrying strains and other strain(s) without limb malformation.

In addition to the *Plzf* coding sequence (Šeda et al., 2005), we determined the coding sequence of *Htr3a* and *Htr3b*, although their involvement in regulation of limb development is improbable—they are expressed and function mainly in the central and peripheral nervous system (Thompson and Lummis, 2007). Coding sequence of *Htr3a* does not contain any variation. There are 3 coding SNPs (single nucleotide polymorphisms) in *Htr3b*, two silent (A352A, L417L) and one missense (H364R). In all three SNPs, the variant present in the *Lx* carrying strains is shared by other nonrelated wild-type rat strains (SD, HTG, and Wistar “BioTest”, see the Experimental Procedures section and Supp. Table S1, which is available online). L417L is a known SNP (dbSNP: rs8155004), H364R is contained in Celera BN – SD

whole genome shotgun comparison (Supp. Table S1) and also in mRNA AF155044 from SD strain. None of the identified variants can thus explain the *Lx* phenotype.

Identification of Putative Functionally Important Noncoding Sequences

Because there is no solid evidence of presence of transcription activity other than the three above-mentioned genes in the 177-kb segment (Fig. 4A, see RefSeq and spliced expressed sequence tag tracks), and there is also no miRNA gene (data not shown), we set to find the potential regulatory elements. According to evolutionary conservation of limb development and structure in vertebrates, we presumed the regulatory sequences would be likely conserved at a similar level. Preformed conservation data for the rat genome are available at UCSC Genome Browser (URL), generated by PhastCons (Siepel et al., 2005) on sequence alignments created by MULTIZ (Blanchette et al., 2004). We

selected conserved noncoding elements (CNEs) for sequencing based on two criteria: (1) PhastCons score and (2) visual inspection of the depth of conservation (in mammals, in terrestrial vertebrates, in all vertebrates). We selected 31 CNEs throughout the differential segment. All elements with PhastCons logarithm of odds (LOD) score > 70 were included, as well as all those conserved at least in mammals and birds. Also, we determined the DNA sequence near the transcription start sites of the three genes (containing the promoters, possible short-range regulatory elements, and 5' untranslated regions [UTRs]) and also 3' UTRs. In total, including the determined coding sequences, we obtained 30 kb of high-quality sequence from each of the PD, PD5, BN, and SHR strains, corresponding to 17% of the 177-kb nonrecombinant segment (Fig. 4A, see coverage track).

Sequence Variation in the Noncoding Sequences

Beyond the 3 previously reported coding SNPs in *Plzf* (Šeda et al., 2005), and 3 coding SNPs in *Htr3b*, we identified 70 sequence variants (Fig. 4A and Supp. Table S1). There are 47 substitutions or SNPs in strict sense; 22 small indels (insertions and deletions up to 14 bp), from which 12 appear to be in a single base “run” and 5 in more complex microsatellites. In addition, during the positional cloning efforts, we identified 6 microsatellites polymorphic between the *Lx*-carrying and other strains (not included in the 70 variants). Last but not least, there is one substantial deletion—2,964 bp in intron 2 of *Plzf* (Fig. 4B,C). Of interest, only 11 of these variants were recognized previously (Supp. Table S1), all the others are novel.

Next, we examined whether the sequence variant was unique for strains carrying the *Lx* mutation. In the majority of cases, we found at least one strain with normal limb development that has identical sequence variant as *Lx* carrying strains. We excluded such variants from further analysis.

We also examined the polymorphic sites in the F2 recombinants for extra fine mapping of the recombination break-points. In this manner, we further re-

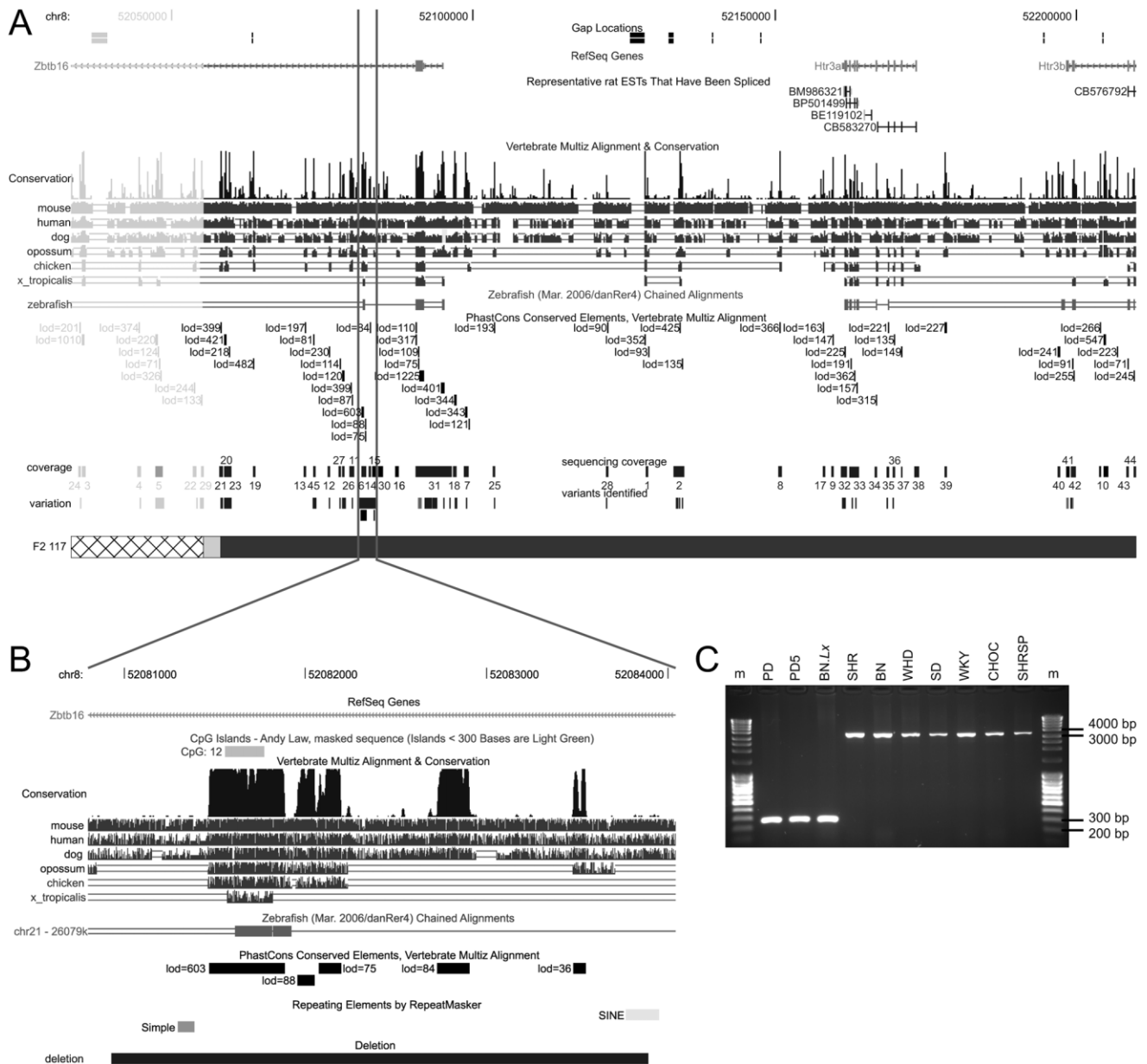


Fig. 4. Nonrecombinant segment, sequencing and variation. **A:** Genome view of the 177 kb *Lx* segment (between 21652 and 21829). Annotation tracks are shown as follows: Gaps; RefSeq genes; spliced expressed sequence tags, only nonredundant included; Conservation by MULTIZ, overall conservation ("Conservation" label on the left), followed by pairwise conservation with individual genomes; *x_tropicalis* = *Xenopus tropicalis*; conservation with zebrafish (not included in MULTIZ alignment); PhastCons conserved elements, only those with LOD score > 70 shown; sequencing coverage of this study, the individual sequenced fragments numbered; variation identified in this study, the magnification does not always allow to match the genomic position exactly, exact positions are listed in Supp. Table S1; chromosome of F2 hybrid 117—SNPs in fragments 24, 3, 4, 5, 22, and 29 are heterozygous in this *Lx* mutant animal, excluding thus the 22-kb segment; corresponding genome features are gray. Crossing-over in F2 117 occurred between fragment 29 and 21 (dark gray on the F2 chromosome). Detailed view of the 177-kb segment with additional annotation tracks can be obtained from UCSC Genome Browser Internet page. The respective coordinates are chr8:52033239–52209946, rat genome assembly version November 2004 (version 3.4 of the Rat Genome Sequencing Consortium). **B:** Expanded view of the region amplified by the polymerase chain reaction in C. Black rectangle at the bottom represents the 2,964 bp deletion in *Lx* mutants. Deletion coordinates are chr8: 52080930–52083893. Additional tracks not shown in A depict CpG islands and repeats by RepeatMasker. **C:** A 2,964-bp deletion in intron 2 of *Plzf* is present only in *Lx*-carrying strains. A 3,240-bp fragment is amplified from wild-type rats, 276 bp from *Lx/Lx* animals. m = molecular weight marker.

duced the nonrecombinant region to 155 kb (Fig. 4A). This criterion leads to absolute exclusion of 9 SNPs and 4 indels.

The only remaining candidate for *Lx* is the 2,964-bp deletion (Fig. 4B,C).

The 2,964-bp Deletion

The 2,964-bp deletion in intron 2 of *Plzf* was found exclusively in rats carrying the *Lx* mutation and was absent

in all other rat strains examined (Fig. 4B,C and data not shown). The deletion removes three CNEs, two moderately conserved and one highly conserved. The most conserved CNE has

PhastCons LOD score 603 (second highest in the 155-kb segment after the exon 2 of *Plzf*), and is conserved in all major vertebrate phyla (where genome comparison is available, Fig. 4A).

Decreased *Plzf* Expression in *Lx/Lx* Limb Buds

Plzf expression in wild-type (WT, +/+) and heterozygotes (+/Lx) was comparable both in pattern and quantity (compare Fig. 5A,D,G to Fig. 5B,E,H). In wild-type rat embryos, *Plzf* expression in limb buds was already established at 12.5 days post coitum (dpc; Fig. 5A). The expression spanned most of the limb bud mesenchyme. At 13.5 dpc in the forelimb bud (Fig. 5D), the expression receded from the tip of the limb bud and split, so the pattern resembled a fork in the middle of the limb bud. In the hindlimb bud, most of the mesenchyme was positive for *Plzf* mRNA, similar to 12.5 dpc. At 14.5 dpc (Fig. 5G), when the autopod was clearly differentiated, *Plzf* signal disappeared from the autopod, but remained in the more proximal portion (future zeugopod) in both fore- and hindlimb buds, being more intense in the hindlimb buds. At 15.5 dpc, the *Plzf* expression in both fore- and hindlimb buds was almost completely gone, with the exception of a weak staining in the proximal part of the hindlimb (data not shown). In addition to limb buds, *Plzf* expression was detectable in many other structures: developing central nervous system (CNS; throughout both brain and spinal cord), branchial arches, mesonephros, and the eye.

In *Lx/Lx* embryos, *Plzf* expression in limb buds was greatly reduced, while staining in the CNS showed pattern and intensity similar to control embryos. At 12.5 dpc (Fig. 5C) the expression was barely detectable in both limb buds, suggesting later expression onset. At 13.5 dpc (Fig. 5F) the expression was reduced, especially in the anterior mesenchyme of the hindlimb. At 14.5 dpc (Fig. 5I) in the forelimb, signal was absent in the zeugopod, and suppressed in the autopod. In the hindlimb, the autopod was negative (as it was in controls), but the zeugopod signal was greatly reduced. At 15.5 dpc, *Plzf* expression became un-

detectable in both fore- and hindlimbs (data not shown).

Confirmation of Decreased *Plzf* Expression by Quantitative Real-Time Polymerase Chain Reaction

We assessed the expression in limb buds also by quantitative real-time polymerase chain reaction (qPCR) with Taqman probes at 12.5 dpc and 13.5 dpc. *Lx/Lx* animals had decreased expression to 20–40% of the levels found in the wild-type (+/+). Heterozygotes showed significantly higher expression than mutant homozygotes, but lower than the wild-type rats (Fig. 6). We used the tail portion of the embryo, containing *Plzf*-expressing neural tube as the positive control. The relative expression level of *Plzf* was slightly higher there than in the WT hindlimb buds, and there was no significant difference among genotypes (data not shown).

Plzf Target Genes Exhibit Changes of Expression Pattern

Next, to assess the functional importance of decreased *Plzf* expression in the *Lx/Lx* limb buds, we examined expression profiles of known *Plzf* targets. Because *Plzf* is a direct repressor of posterior *HoxD* genes (Barna et al., 2002), we focused on *Hoxd10–Hoxd13*.

Forelimbs, which do not have any skeletal phenotype, showed no difference in *HoxD* expression pattern in *Lx/Lx* embryos compared with +/Lx at all stages examined (data not shown). There was also no change of expression in hindlimbs at 12.5 (not shown) and 13.5 dpc (Fig. 7A–D). The 13.5 dpc marks an end of the first *HoxD* expression phase. However, at 14.5 dpc (Fig. 7A–D), *Hoxd10–13* expression in the *Lx/Lx* hindlimb buds was extended into the anterior portion of the autopod. At the same stage, the mutant phenotype became distinguishable morphologically in the form of an enlargement of the anterior part of the autopod. *Hoxd10* and *Hoxd11* that are also expressed in the presumable zygo pod, showed an enlarged expression domain in the anterior half of *Lx/Lx* zeugopod, resulting in a nearly

Fig. 5. Expression of *Plzf* throughout the limb development. Whole-mount RNA in situ hybridization of *Plzf* at 12.5 days post coitum (dpc) to 14.5 dpc embryos. **A,D,G:** wild-type (+/+) embryos. **B,E,H:** +/Lx embryos (displaying wild-type feet), **C,F,I:** *Lx/Lx* embryos. In all stages observed, *Plzf* expression in the mutant limb buds is markedly decreased in comparison to both +/Lx and +/+ limbs. We did not observe marked differences between +/Lx and +/+ limb buds. Note that, at 14.5 dpc, the future preaxial polydactyly in *Lx/Lx* (F) became already distinguishable by enlargement of the anterior part of the autopod. Scale bars = 1 mm.

symmetrical A–P pattern, in contrast to the marked asymmetry in control limb buds (Fig. 7A,B).

We further examined the expression of *Shh* (Fig. 7E), because alterations of *Shh* function are involved in many models of preaxial polydactyly. There was no change of *Shh* expression in mutant limb buds in comparison to controls. Specifically, *Shh* expression in the mutants remained confined to the posterior ZPA with no signs of changed or ectopic expression.

Bmp2 (Fig. 7F) was expressed in the hindlimb bud mesenchyme at 13.5 dpc in a small area close to the posterior margin with no difference between mutant and control embryos. In the hindlimbs of both control and mutant embryos at 14.5 dpc, there was similar marked positivity in the presumptive third interdigital space, as well as in the clearly demarcated fourth space. The first and second interdigital spaces were not fully developed yet, and showed only moderate level of *Bmp2* mRNA. In *Lx/Lx* embryos, there was an additional large peak of expression extending to the most anterior tip of the limb bud. Expression in the posterior autopod/zeugopod was not changed.

In summary, the expression data show reduced *Plzf* expression in the limb bud, especially in its anterior portion, resulting in anterior expansion of *HoxD* signaling.

DISCUSSION

Plzf expression pattern in wild-type rats is comparable with expression of the orthologous gene in the mouse (Avantaggiato et al., 1995; Cook et al., 1995), including the limb bud expres-

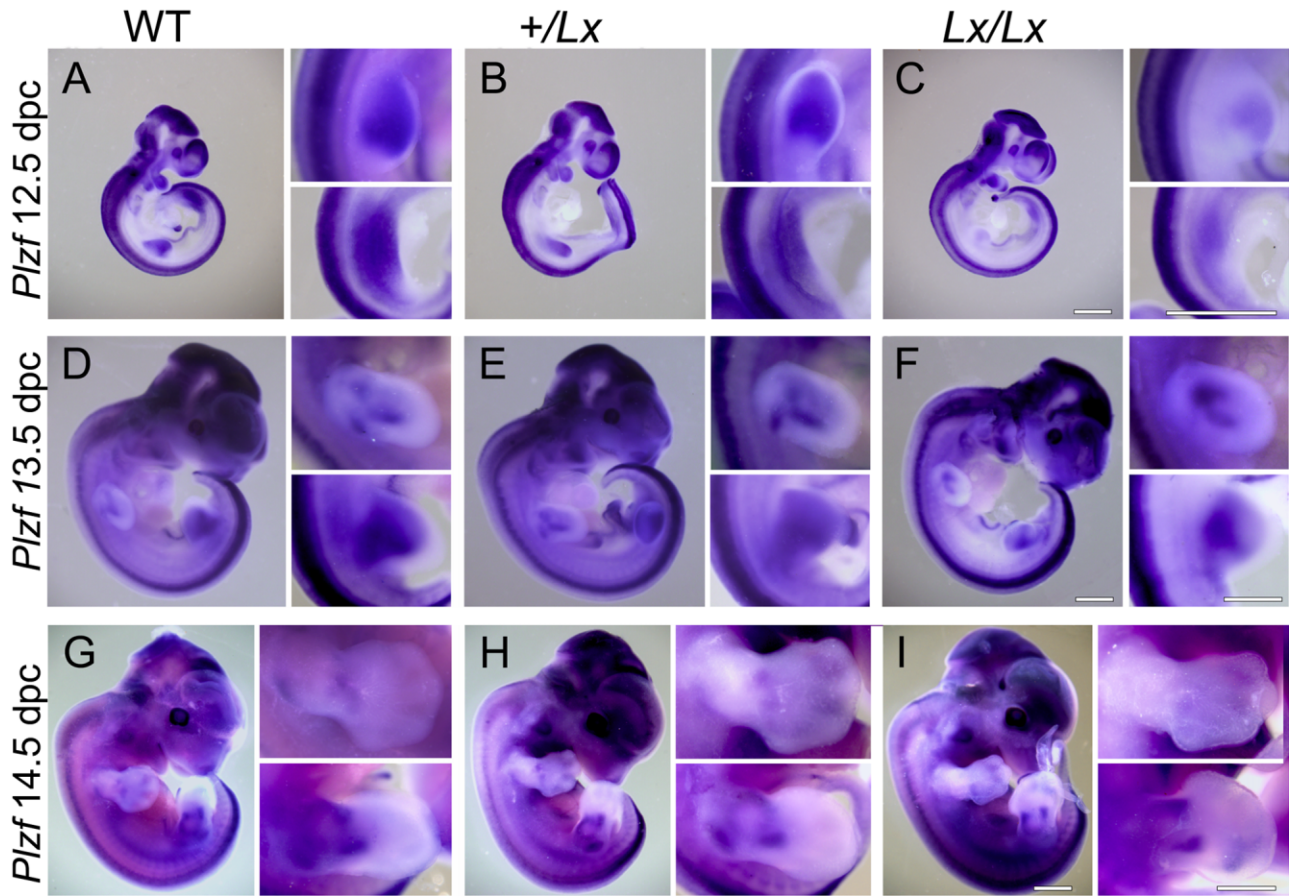


Fig. 5.

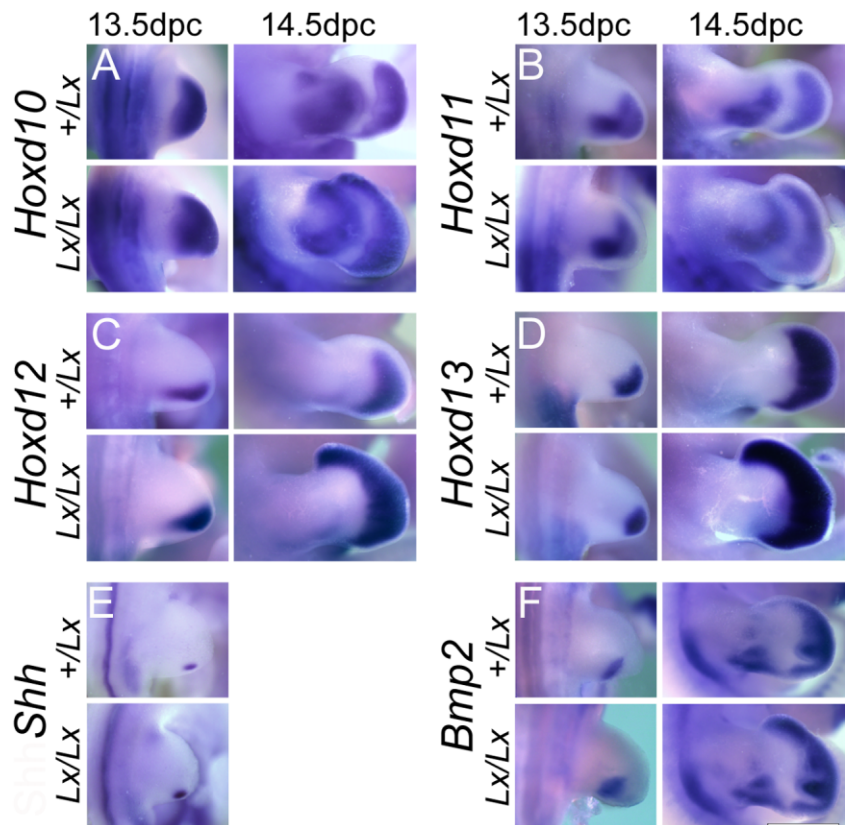


Fig. 7. Expression of *Plzf* target genes during hind limb development. Whole-mount RNA in situ hybridization. The top margin and bottom margin denote the anterior and posterior parts of the limb, respectively, in all panels. A–D: Whole-mount in situ hybridization of *Hoxd10–13* genes at 13.5 days post coitum (dpc) and 14.5 dpc in *Lx/Lx* and *+Lx* controls. *HoxD* gene expression is altered in *Lx/Lx* embryos. **A:** *Hoxd10* expression in hindlimbs is extended anteriorly both in autopod and zygotid at 14.5 dpc. Autopod already shows signs of accumulation of extra material, delineating the future polydactyly. **B:** Similar findings characterize *Hoxd11* expression at 14.5, the changed expression pattern is preserved at least up to 15.5 dpc (not shown). **C,D:** *Hoxd12* (C) expression in autopod at 14.5 dpc is “anteriorized” in a manner comparable to other posterior *HoxD* genes, the same is true for *Hoxd13* at 14.5 (D). **E:** Whole-mount in situ hybridization of *Shh* at 13.5 dpc in *Lx/Lx* and *+Lx* controls. No difference in *Shh* expression can be found between *Lx/Lx* and *+Lx* embryos (13.5 dpc), at 14.5 dpc *Shh* signal is already absent (data not shown). **F:** Whole-mount in situ hybridization of *Bmp2* at 13.5 dpc and 14.5 dpc in *Lx/Lx* and *+Lx* controls. *Bmp2* expression is anteriorized in similar way to *Hoxd10–13*. Scale bars = 1 mm.

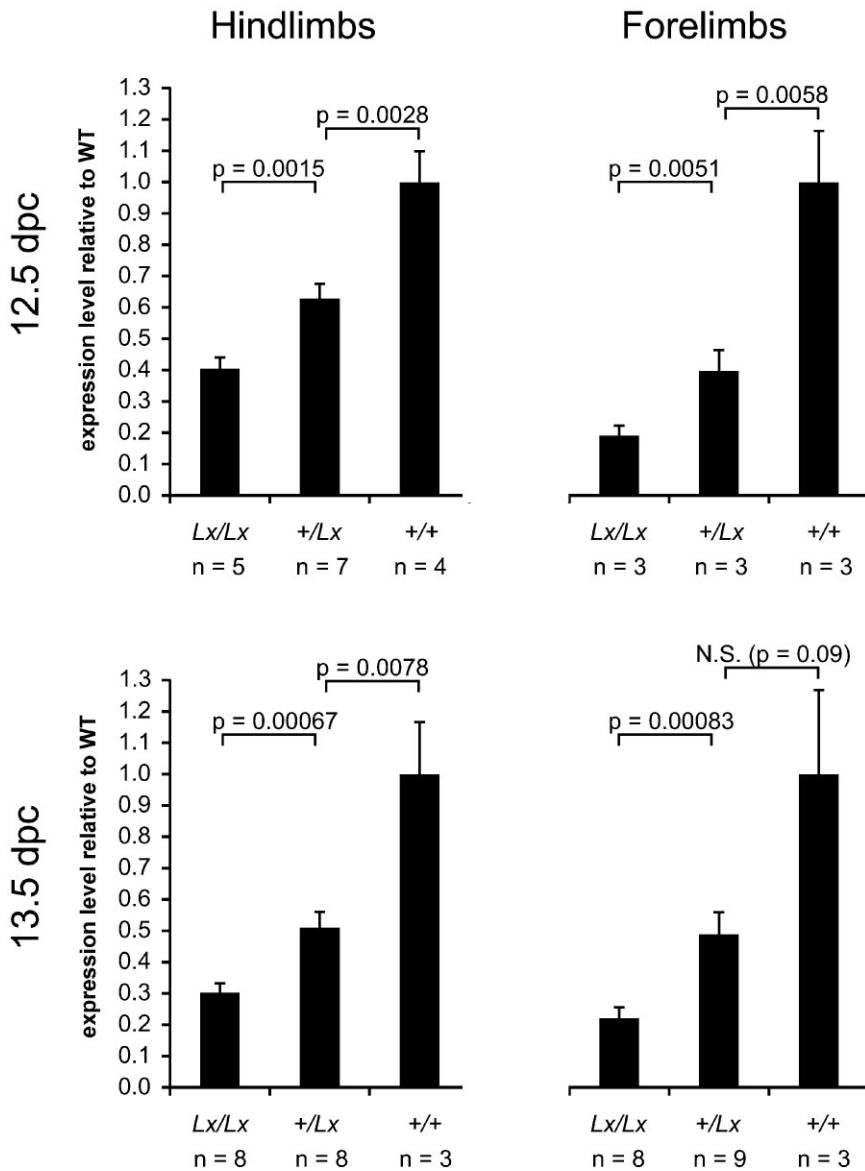


Fig. 6. *Plzf* expression evaluation in limb buds by quantitative polymerase chain reaction (qPCR) at 12.5 and 13.5 days post coitum (dpc). Expression was assessed by a Taqman localized at the most 5' exon junction. However, we obtained similar results with second Taqman probe at exon 5 to 6 junction. Each sample represents a pool of both fore- or hindlimbs respectively, from the given embryo. The number of unique samples is given under each column. Columns represent means \pm SEM of expression level relative to wild-type (WT). *P* values (above columns) represent significance levels of Tukey post hoc tests modified for unequal *n* between the indicated groups. The statistical analysis was performed on ddCt values instead of the relative expression which is shown in the graph (see the Experimental Procedures section). Mutant limb buds at both stages have significantly lower *Plzf* expression compared with WT (20–40%). Heterozygotes show intermediate expression levels, consistent with the proposed *cis*-acting nature of the deleted *Plzf* intron 2 sequence.

sion. In *Lx/Lx* mutant rats, there are substantial changes in the *Plzf* expression pattern in the limb buds, while the expression in other structures is comparable to the wild-type. This can explain why the *Lx* phenotype is restricted to limb, whereas *Plzf*^{-/-} mice display affliction of the axial skeleton and defective spermat-

ogenesis. In PD5 rats, forelimbs are not affected despite the changes in *Plzf* expression present in both fore- and hindlimbs. We cannot fully account for this phenomenon. There may be functional redundancy due to the fact that the forelimb bud expresses a *Plzf* homolog (Davies et al., 1999). In any case, restriction of the

mutant phenotype to hindlimbs was observed also in *Plzf*^{-/-} mice (Barna et al., 2000) and *Plzf*^{-/-} *Gli3*^{-/-} double null mice (Barna et al., 2005). In heterozygotes (+/*Lx*), in situ hybridization (ISH) data show *Plzf* expression comparable to +/+. However, in qPCR, the expression is lower in the heterozygotes. Presumably, the difference is due to greater sensitivity of qPCR enabling detection of slight changes in expression. Nevertheless, the qPCR result is in accord with the character of the mutation—regulatory elements in DNA normally act only in *cis*, predictive of intermediate expression levels in heterozygotes compared with both homozygote types.

Plzf^{-/-} mice displayed a relatively wide spectrum of hindlimb phenotypes, afflicting all three limb segments (stylopod–autopod). In the digital arch, the following phenotypes were noted: triphallangeal hallux, with or without an additional preaxial digit, or missing hallux. Zeugopod showed separation of tibia and fibula, thickening of fibula and shortening of the whole zeugopod. Rarely, forelimbs were also affected in a corresponding manner (Barna et al., 2000). PD5 displays only limited autopod phenotype variation (Fig. 1). This may be the result of a hypomorphic nature of *Lx* mutation (up to 40% of WT *Plzf* expression level is preserved in the mutants). Such interpretation is corroborated by the fact that we observed an alteration of the second phase of *HoxD* expression, but not of the early first phase in *Lx/Lx* rats, whereas in *Plzf*^{-/-} mice, both phases are affected.

In contrary to the *Plzf*^{-/-} phenotype, which was analyzed on a mixed genetic background, PD5 is an inbred strain. Therefore, the phenotype of the *Lx/Lx* homozygotes may be stabilized at a certain severity by the uniform genetic background. Indeed, gross phenotype of other strains containing the *Lx* allele (Printz et al., 2003) supports this hypothesis. In BN.*Lx*, another congenic strain (with genetic background different from PD5, albeit also uniform), we observed 6-toed hindlimbs, shortening of the hindlimb zeugopod with distal bending and fibula thickening. The forelimbs had a well-developed thumb (in wild-type rats, thumb is rudimentary). More-

over, in BN.*Lx* × BN cross, hindlimb polydactyly (6 toes) is present in approximately 60% of the heterozygous offspring (Kren, 1975). This does not change the fact that, in the experimental setting of this study, using SHR genetic background, *Lx* behaves as strictly recessive. Moreover, *Lx* mutation segregates in the largest rat recombinant inbred (RI) strain panel HXB and BXH (Printz et al., 2003). Each RI strain, derived by inbreeding of a F2 progeny, represents a unique, but reproducible, combination of the parental genomes (for BXH and HXB panels, parents are SHR and BN.*Lx*). There are 31 HXB and BXH strains including 1 subline; 19 strains and the subline are *Lx/Lx* homozygotes, with reproducible limb phenotypes for each strain, but a huge interstrain variation. For example, the BXH2 strain presents with forelimb polyphalangy (5 triphalangeal digits), missing thumbs in hindlimbs (4 digits), and hindlimb zeugopod affliction more pronounced than in BN.*Lx*. On the other pole of the variation spectrum, we can name BXH3, with limb phenotype resembling PD5. This limb phenotype spectrum is matching surprisingly well to the phenotype spectrum observed in the *Plzf*^{-/-} mice.

We showed that *Lx* influences limb patterning independently of Shh. In contrast, the changes in posterior *HoxD* gene expression indicate that *HoxD* genes are among the effectors leading to polydactyly in *Lx/Lx* rats. This finding corresponds well to analysis of the *Plzf*^{-/-} mice (Barna et al., 2000) that showed similar changes in expression of *HoxD* genes. The relationship of *Shh* and *HoxD* genes is complex and supposedly different for the first and the second phase of *HoxD* expression (Tarchini and Duboule, 2006). It is not surprising as these two phases occur before and after Shh signaling. The first phase of *HoxD* expression, especially the restriction of *Hoxd10–13* expression in the posterior part of developing limb bud, is essential for triggering expression of *Shh* and maintaining correct *Shh* expression posteriorly in the ZPA (Zakany et al., 2004). In contrast, the second phase of *HoxD* (*Hoxd10–13*) expression in developing autopod is supposed to be induced or at least modulated by Shh or by its counter-

player, Gli3 (Zuniga and Zeller, 1999). As our and other's (Barna et al., 2000) works show, despite correct *Shh* expression in *Lx/Lx* rats or *Plzf*^{-/-} mice, *HoxD* expression is anteriorized, resulting in preaxial polydactyly. We can conclude that *Plzf* might be a mediator of the Shh effect on *HoxD* genes or *Plzf* and Shh might be two independent factors co-defining the autopod *HoxD* expression pattern. The second possibility seems to reflect the reality better in the light of the findings of Barna et al. (2002). These investigators addressed a question why *Plzf* represses *Hoxd10–13* expression only in the anterior region, while its expressions extends almost throughout the limb bud. They showed that the repressive ability of *Plzf* is antagonized in posterior regions of the limb by signals such a retinoid acid and Shh. In accordance with these findings, it seems that a total absence of *Plzf* (in -/- mice) and reduced expression of *Plzf* in the anterior part of the limb bud (in *Lx/Lx* rats at 13.5 dpc, Fig. 4D) can be functionally equal and can elicit the same phenotype. Alternatively, phenotypic equivalence of *Plzf*^{-/-} and *Lx/Lx* can be due to later onset of *Plzf* expression in *Lx/Lx* limb buds, pointing to possible importance of *Plzf* for the autopod at earlier stage (12.5 dpc, Fig. 4B).

The amount of programmed cell death is reduced both in *Lx/Lx* rats (Sedmera et al., 1998) and *Plzf*^{-/-} mice (Barna et al., 2000). As *Bmp2* is supposed to be a modulator or even a trigger of programmed cell death, we expected its reduced expression in *Lx/Lx* compared with control. Surprisingly, the only difference we observed is anteriorization of *Bmp2* expression in *Lx/Lx* embryos, in a manner similar to posterior *HoxD* genes.

The involvement of *Plzf* in limb patterning is well documented in the mouse, thanks to analysis of *Plzf*^{-/-} animals (Barna et al., 2000, 2002, 2005). The major novel finding of our study is the identification of a putative *cis*-acting *Plzf* regulator that may enable us to detect genes acting upstream of *Plzf*. Our data suggest that the regulatory element in question resides in the 2,964-bp deletion. The deleted sequence contains the most highly conserved noncoding sequence element, and the conservation is also

the deepest (fish–mammals) in the region. This is in agreement with our hypothesis stating that sequence necessary for proper limb development should be conserved at least in terrestrial vertebrates, possibly even in fish (as fish fins share many common aspects with tetrapod limb development). Compared with other sequence variants (mainly SNPs) identified in the nonrecombinant region, only the deletion is exclusively associated with *Lx*. The only alternative explanation of *Lx* can be a missed sequence variant in the part of the segment that was not sequenced. However, this would be greatly surprising, as this part is not conserved.

A limb-bud-specific, long-range regulatory element driving sonic hedgehog (*Shh*) expression in the ZPA was described previously (Lettice et al., 2002). The *Shh* regulatory *cis*-acting element was characterized in detail (Lettice et al., 2003, 2007; Lettice and Hill, 2005). The importance of the *Shh* regulator is underscored by its point mutations responsible for human preaxial polydactyly (Lettice et al., 2007). The element identified in this study is not similar at the DNA level to the long range *Shh* regulator. This is not surprising, as the expression patterns of *Shh* (in ZPA) and *Plzf* (almost everywhere in the limb bud mesenchyme) are dissimilar. Another example of dissection of a regulatory region involved in limb development was provided by the mouse mutation *limb deformity* (*ld*), which is caused by disruption of a “global control region” for *gremlin* expression (Zuniga et al., 2004).

Our study presents the first evidence of possible molecular mechanism acting during the limb development to produce the *Lx* phenotype. Further analysis of the deletion would be necessary to confirm the role of the deleted CNE in limb development, e.g., by creating transgenic animals with reporter gene expression driven by the deleted element. It may be interesting to investigate whether the deleted element is a selective regulator of *Plzf* expression in the limb bud, given the many processes where *Plzf* is involved. At this stage, it seems that the regulator is not essential for the spermatogenic stem cells, as the *Lx/Lx* males have normal fertility.

The CNS expression of *Plzf* is also unchanged in the *Lx/Lx* embryos. The deletion (2,964 bp) is too long for reliable prediction of which of the many potential transcription factor binding sites are functionally important. Moreover, the deletion contains not one, but several CNEs with varying conservation depth. To further decipher *Plzf* regulation through the deleted sequence, it will be necessary to perform functional studies of enhancer properties of deletion variants of the element.

EXPERIMENTAL PROCEDURES

Animals and Linkage Mapping

In this study, following rat strains were used: inbred strain SHR/OlaIpcv, RGD (Rat Genome Database) ID: 631848; inbred strain BN/Cub, RGD ID: 737899; congenic strain SHR.*Lx*.PD5, RGD ID: 1641851 (PD5 hereafter). For sequencing, we also used DNA isolated from: PD/Cub, RGD ID: 728161; BN.PD-(D8Rat39-D8Rat35)/Cub, RGD ID: 728144 (BN.*Lx* hereafter); CHOC/Cub, RGD ID: 737958; SD, RGD ID: 70508; SHRSP/Bbb, RGD ID: 1581618; WKY/Bbb, RGD ID: 1581635 (SHRSP and WKY DNA is kind gift of N. Hubner of MDC Berlin); HTG, RGD ID: 1302795 (kind gift of J. Kuneš, Institute of Physiology, Praha); a second colony of HTG (kind gift of L. Kazdová, IKEM Praha); outbred Wistar from Velaz Ltd., Czech Republic; outbred Wistar from BioTest Ltd., Czech Republic; WHD (Wistar hypodactylous, Liška et al., unpublished results). In addition to various Wistar rats, SHR, SHRSP, WKY, WHD, and HTG are derived from outbred Wistar rat colonies, as is PD.

All experiments were performed in agreement with the Animal Protection Law of the Czech Republic (311/1997) which is in compliance with the European Community Council recommendations for the use of laboratory animals 86/609/ECC. All experiments were approved by The Charles University Animal Care Committee.

For ISH, we used PD5 (mutant) and SHR as a wild-type control. To obtain littermates with different genotypes,

SHR was crossed to PD5, and the resulting F1 hybrids were intercrossed to obtain all possible genotypes of the *Lx* locus in F2 littermates (*Lx/Lx*, *+/Lx*, *+/+*).

For linkage mapping, we generated F2 (PD5 × BN) hybrids, *n* = 247. We assessed their limb phenotype visually after birth. We isolated genomic DNA from the tail by phenol-chloroform extraction and ethanol precipitation, subjected it to amplification by standard PCR technique, and analyzed the products on native polyacrylamide gel electrophoresis stained with ethidium bromide. Primers for PCR correspond to established microsatellite markers in the PD5 differential segment: D8Rat42, D8Got72, D8Rat94, and D8Arb23. We also searched for additional microsatellites by Pompous (Fondon et al., 1998) or used preformatted trf (Benson, 1999) data available through UCSC Genome Browser. We designed primers flanking microsatellites using Primer3 (Rozen and Skaletsky, 2000), the amplicons were tested for length polymorphism. Primers for polymorphic microsatellites are listed in Supp. Table S2. We also determined, using sequencing, the genotype of F2 No. 110 in the interval between 21807 and 21829 bp; and No. 117 in the interval between 21652 bp and D8Got72 respectively, to map the crossing-over events with highest precision. While in the former case there was no reduction of the candidate region, analysis of no. 117 led to exclusion of 22 kb from the candidate region.

Search for CNEs

We inspected the nonrecombinant *Lx* carrying segment using UCSC genome browser. It contains preformed alignment with other vertebrate genomes, generated by MULTIZ (Blanchette et al., 2004), and the most conserved elements identified and scored by PhastCons (Siepel et al., 2005). Our (initial) inclusion criteria for sequencing were PhastCons LOD score > 70, or conservation at least among mammals and birds.

Sequencing

Tail genomic DNA was amplified by PCR with specific primers (Supp. Ta-

ble S2). PCR fragments were analyzed by electrophoresis and sequenced directly using PCR primers and BigDye Terminator v1.1 Cycle Sequencing Kit (Applied Biosystems, Foster City, CA) and the sequencing products analyzed using ABI PRISM 310 Genetic Analyzer (Applied Biosystems). DNA sequences were deposited in GenBank, dbSTS, and the variation in dbSNP (pending).

Whole-Mount ISH

Probes were generated from RT-PCR products (primers see Supp. Table S2). RNA was isolated from adult heart (in case of *Plzf*) or from whole embryos at 12.5 dpc (*Hoxd10-13*, *Bmp2*, *Shh*). PCR products were cloned into pDrive (Qiagen, Valencia, CA) or pCR-Blunt-TOPO (Invitrogen, Carlsbad, CA). Sense/Antisense RNA was synthesized by in vitro transcription using SP6 or T7 RNA polymerase, with appropriate promoters present in the vector.

The ISH on whole-mount embryos was performed as described (Nieto et al., 1996). Briefly, embryos were fixed in 4% paraformaldehyde in phosphate buffered saline with 0.1% Triton X-100 overnight at 4°C, and then transferred into methanol. Hybridization was performed with digoxigenin labeled antisense riboprobes at 70°C over 1–2 days. Fab fragments of sheep antibody to digoxigenin conjugated to alkaline phosphatase mediated the visualization (1:5,000, Roche), *n* > 4 for each stage/genotype, in at least two independent replicates. The compared embryos of *+/+*, *+/Lx*, and *Lx/Lx* genotypes were hybridized in the same reaction, using identical hybridization mixture and equal staining time.

The qPCR

RNA was isolated from limb buds (fore- and hindlimb buds were pooled for each embryo) and tail by RNeasy Mini Kit (Hilden, Germany) according to manufacturer instructions, and reverse transcribed by SuperScript III (Invitrogen) using random hexamer primers.

Taqman probes were purchased from Applied Biosystems. *Plzf* assay spans exons 1-2 (assay ID Rn01418641_m1). We also used a probe/primer set amplifying

exon 5–6 junction (Rn01418644_m1). GAPDH (catalog no. 4308313) was used as control. Samples were run on Applied Biosystems Real-time PCR System 7000. Each sample represented a pool of both fore- and hindlimb buds of the given embryo. Each sample was run in quadruplicate. Relative expression levels were computed using standard ddCt method, expression level in $+/+$ animals was set to 1. Statistical significance was determined on ddCt values using STATISTICA by analysis of variance, between group differences computed by Tukey Honest Significant Difference test modified for unequal N. The ddCt values instead of relative expression values were used because of their normal distribution.

REFERENCES

- Avantaggiato V, Pandolfi PP, Ruthardt M, Hawe N, Acampora D, Pelicci PG, Simone A. 1995. Developmental analysis of murine Promyelocyte Leukemia Zinc Finger (PLZF) gene expression: implications for the neuromeric model of the forebrain organization. *J Neurosci* 15:4927–4942.
- Bardwell VJ, Treisman R. 1994. The POZ domain: a conserved protein-protein interaction motif. *Genes Dev* 8:1664–1677.
- Barna M, Hawe N, Niswander L, Pandolfi PP. 2000. *Plzf* regulates limb and axial skeletal patterning. *Nat Genet* 25:166–172.
- Barna M, Merghoub T, Costoya JA, Ruggero D, Branford M, Bergia A, Samori B, Pandolfi PP. 2002. *Plzf* mediates transcriptional repression of *HoxD* gene expression through chromatin remodeling. *Dev Cell* 3:499–510.
- Barna M, Pandolfi PP, Niswander L. 2005. *Gli3* and *Plzf* cooperate in proximal limb patterning at early stages of limb development. *Nature* 436:277–281.
- Benson G. 1999. Tandem repeats finder: a program to analyze DNA sequences. *Nucleic Acids Res* 27:573–580.
- Blanchette M, Kent WJ, Riemer C, Elnitski L, Smit AF, Roskin KM, Baertsch R, Rosenbloom K, Clawson H, Green ED, Haussler D, Miller W. 2004. Aligning multiple genomic sequences with the threaded blockset aligner. *Genome Res* 14:708–715.
- Buaas FW, Kirsh AL, Sharma M, McLean DJ, Morris JL, Griswold MD, de Rooij DG, Braun RE. 2004. *Plzf* is required in adult male germ cells for stem cell self-renewal. *Nat Genet* 36:647–652.
- Cook M, Gould A, Brand N, Davies J, Strutt P, Shaknovich R, Licht J, Waxman S, Chen Z, Gluecksohn-Waelsch S, et al. 1995. Expression of the zinc-finger gene *PLZF* at rhombomere boundaries in the vertebrate hindbrain. *Proc Natl Acad Sci U S A* 92:2249–2253.
- Costoya JA, Hobbs RM, Barna M, Cattorretti G, Manova K, Sukhwani M, Orwig KE, Wolgemuth DJ, Pandolfi PP. 2004. Essential role of *Plzf* in maintenance of spermatogonial stem cells. *Nat Genet* 36:653–659.
- David G, Alland L, Hong SH, Wong CW, DePinho RA, Dejean A. 1998. Histone deacetylase associated with mSin3A mediates repression by the acute promyelocytic leukemia-associated *PLZF* protein. *Oncogene* 16:2549–2556.
- Davies JM, Hawe N, Kabarowski J, Huang QH, Zhu J, Brand NJ, LePrince D, Dhordain P, Cook M, Morriss-Kay G, Zelent A. 1999. Novel BTB/POZ domain zinc-finger protein, LRF, is a potential target of the *LAZ-3/BCL-6* oncogene. *Oncogene* 18:365–375.
- Dong S, Zhu J, Reid A, Strutt P, Guidez F, Zhong HJ, Wang ZY, Licht J, Waxman S, Chomienne C, Chen Z, Zelent A, Chen SJ. 1996. Amino-terminal protein-protein interaction motif (POZ-domain) is responsible for activities of the promyelocytic leukemia zinc finger-retinoic acid receptor- α fusion protein. *Proc Natl Acad Sci U S A* 93:3624–3629.
- Felicetti F, Bottero L, Felli N, Mattia G, Labbaye C, Alvino E, Peschle C, Colombo MP, Care A. 2004. Role of *PLZF* in melanoma progression. *Oncogene* 23:4567–4576.
- Fischer S, Kohlhasse J, Bohm D, Heitmann M, Schweiger B, Hoffmann D, Horsthemke B, Wiczorek D. 2008. Biallelic loss of function of the promyelocytic leukemia zinc finger (*PLZF*) gene causes severe skeletal defects and genital hypoplasia. *J Med Genet* 45:731–737.
- Fondon JW, 3rd, Mele GM, Brezinschek RI, Cummings D, Pande A, Wren J, O'Brien KM, Kupfer KC, Wei MH, Lerman M, Minna JD, Garner HR. 1998. Computerized polymorphic marker identification: experimental validation and a predicted human polymorphism catalog. *Proc Natl Acad Sci U S A* 95:7514–7519.
- Galis F, van Alphen JJM, Metz JAJ. 2001. Why five fingers? Evolutionary constraints on digit numbers. *Trends Ecol Evol* 16:637–646.
- Graham TJ, Riss AM. 1998. Finger polydactyly. *Hand Clin* 14:49–64.
- He LZ, Guidez F, Tribioli C, Peruzzi D, Ruthardt M, Zelent A, Pandolfi PP. 1998. Distinct interactions of *PML-RAR α* and *PLZF-RAR α* with co-repressors determine differential responses to RA in APL. *Nat Genet* 18:126–135.
- Hong SH, David G, Wong CW, Dejean A, Privalsky ML. 1997. SMRT corepressor interacts with *PLZF* and with the *PML-retinoic acid receptor alpha (RAR α)* and *PLZF-RAR α* oncoproteins associated with acute promyelocytic leukemia. *Proc Natl Acad Sci U S A* 94:9028–9033.
- Kren V. 1975. Genetics of the polydactyly-luxate syndrome in the Norway rat, *Rattus norvegicus*. *Acta Univ Carol Med Monogr* 1–103.
- Kren V, Krenova D, Pravenec M, Zdobinska M. 1995. Chromosome 8 congenic strains: tools for genetic analysis of limb malformation, plasma triglycerides, and blood pressure in the rat. *Folia Biol (Praha)* 41:284–293.
- Kren V, Bila V, Kasperek R, Krenova D, Pravenec M, Rapp K. 1996. Recombinant inbred and congenic strains of the rat for genetic analysis of limb morphogenesis. *Folia Biol (Praha)* 42:159–166.
- Kuijper S, Feitsma H, Sheth R, Korving J, Reijnen M, Meijlink F. 2005. Function and regulation of *Alx4* in limb development: complex genetic interactions with *Gli3* and *Shh*. *Dev Biol* 285:533–544.
- Labbaye C, Spinello I, Quaranta MT, Pelosi E, Pasquini L, Petrucci E, Biffoni M, Nuzzolo ER, Billi M, Foa R, Brunetti E, Grignani F, Testa U, Peschle C. 2008. A three-step pathway comprising *PLZF/miR-146a/CXCR4* controls megakaryopoiesis. *Nat Cell Biol* 10:788–801.
- Lettice LA, Horikoshi T, Heaney SJ, van Baren MJ, van der Linde HC, Breedveld GJ, Joosse M, Akarsu N, Oostra BA, Endo N, Shibata M, Suzuki M, Takahashi E, Shinka T, Nakahori Y, Ayusawa D, Nakabayashi K, Scherer SW, Heutink P, Hill RE, Noji S. 2002. Disruption of a long-range cis-acting regulator for *Shh* causes preaxial polydactyly. *Proc Natl Acad Sci U S A* 99:7548–7553.
- Lettice LA, Heaney SJ, Purdie LA, Li L, de Beer P, Oostra BA, Goode D, Elgar G, Hill RE, de Graaff E. 2003. A long-range *Shh* enhancer regulates expression in the developing limb and fin and is associated with preaxial polydactyly. *Hum Mol Genet* 12:1725–1735.
- Lettice LA, Hill RE. 2005. Preaxial polydactyly: a model for defective long-range regulation in congenital abnormalities. *Curr Opin Genet Dev* 15:294–300.
- Lettice LA, Hill AE, Devenney PS, Hill RE. 2007. Point mutations in a distant sonic hedgehog cis-regulator generate a variable regulatory output responsible for preaxial polydactyly. *Hum Mol Genet* 17:978–985.
- Li JY, English MA, Ball HJ, Yeyati PL, Waxman S, Licht JD. 1997. Sequence-specific DNA binding and transcriptional regulation by the promyelocytic leukemia zinc finger protein. *J Biol Chem* 272:22447–22455.
- Martin PJ, Delmotte MH, Formstecher P, Lefebvre P. 2003. *PLZF* is a negative regulator of retinoic acid receptor transcriptional activity. *Nucl Recept* 1:6.
- Naray-Fejes-Toth A, Boyd C, Fejes-Toth G. 2008. Regulation of epithelial sodium transport by promyelocytic leukemia zinc finger protein. *Am J Physiol Renal Physiol* 295:F18–F26.
- Nieto MA, Patel K, Wilkinson DG. 1996. In situ hybridization analysis of chick embryos in whole mount and tissue sections. *Methods Cell Biol* 51:219–235.
- Niswander L. 2003. Pattern formation: old models out on a limb. *Nat Rev Genet* 4:133–143.
- Parrado A, Robledo M, Moya-Quiles MR, Marin LA, Chomienne C, Padua RA, Alvarez-Lopez MR. 2004. The promyelocytic leukemia zinc finger protein down-regulates apoptosis and expression of the proapoptotic *BID* protein in lympho-

- cytes. *Proc Natl Acad Sci U S A* 101: 1898–1903.
- Piazza F, Gurrieri C, Pandolfi PP. 2001. The theory of APL. *Oncogene* 20:7216–7222.
- Piazza F, Costoya JA, Merghoub T, Hobbs RM, Pandolfi PP. 2004. Disruption of PLZF in mice leads to increased T-lymphocyte proliferation, cytokine production, and altered hematopoietic stem cell homeostasis. *Mol Cell Biol* 24:10456–10469.
- Printz MP, Jirout M, Jaworski R, Alemayehu A, Kren V. 2003. Genetic models in applied physiology. HXB/BXH rat recombinant inbred strain platform: a newly enhanced tool for cardiovascular, behavioral, and developmental genetics and genomics. *J Appl Physiol* 94:2510–2522.
- Riddle RD, Johnson RL, Laufer E, Tabin C. 1993. Sonic hedgehog mediates the polarizing activity of the ZPA. *Cell* 75:1401–1416.
- Rozen S, Skaletsky H. 2000. Primer3 on the WWW for general users and for biologist programmers. *Methods Mol Biol* 132: 365–386.
- Schefe JH, Menk M, Reinemund J, Effertz K, Hobbs RM, Pandolfi PP, Ruiz P, Unger T, Funke-Kaiser H. 2006. A novel signal transduction cascade involving direct physical interaction of the renin/prorenin receptor with the transcription factor promyelocytic zinc finger protein. *Circ Res* 99:1355–1366.
- Sedmera D, Novotna B, Bila V, Kren V. 1998. The role of cell death in limb development of rats manifesting Lx allele on different genetic backgrounds. *Eur J Morphol* 36:173–181.
- Senbonmatsu T, Saito T, Landon EJ, Watanabe O, Price E, Jr., Roberts RL, Imboden H, Fitzgerald TG, Gaffney FA, Inagami T. 2003. A novel angiotensin II type 2 receptor signaling pathway: possible role in cardiac hypertrophy. *EMBO J* 22:6471–6482.
- Sheth R, Bastida MF, Ros M. 2007. Hoxd and Gli3 interactions modulate digit number in the amniote limb. *Dev Biol* 310:430–441.
- Siepel A, Bejerano G, Pedersen JS, Hinrichs AS, Hou M, Rosenbloom K, Clawson H, Spieth J, Hillier LW, Richards S, Weinstock GM, Wilson RK, Gibbs RA, Kent WJ, Miller W, Haussler D. 2005. Evolutionarily conserved elements in vertebrate, insect, worm, and yeast genomes. *Genome Res* 15:1034–1050.
- Sitterlin D, Tiollais P, Transy C. 1997. The RAR alpha-PLZF chimera associated with Acute Promyelocytic Leukemia has retained a sequence-specific DNA-binding domain. *Oncogene* 14:1067–1074.
- Šeda O, Liška F, Šedová L, Kazdová L, Křenová D, Křen V. 2005. A 14-gene region of rat chromosome 8 in SHR-derived polydactylous congenic substrain affects muscle-specific insulin resistance, dyslipidaemia and visceral adiposity. *Folia Biol (Praha)* 51:53–61.
- Talamillo A, Bastida MF, Fernandez-Teran M, Ros MA. 2005. The developing limb and the control of the number of digits. *Clin Genet* 67:143–153.
- Tarchini B, Duboule D. 2006. Control of Hoxd genes' collinearity during early limb development. *Dev Cell* 10:93–103.
- Tarchini B, Duboule D, Kmita M. 2006. Regulatory constraints in the evolution of the tetrapod limb anterior-posterior polarity. *Nature* 443:985–988.
- Thompson AJ, Lummis SC. 2007. The 5-HT3 receptor as a therapeutic target. *Expert Opin Ther Targets* 11:527–540.
- Yang Y, Drossopoulou G, Chuang PT, Duprez D, Marti E, Bumcrot D, Vargesson N, Clarke J, Niswander L, McMahon A, Tickle C. 1997. Relationship between dose, distance and time in Sonic Hedgehog-mediated regulation of anteroposterior polarity in the chick limb. *Development* 124:4393–4404.
- Yeyati PL, Shakhovich R, Boterashvili S, Li J, Ball HJ, Waxman S, Nason-Burchenal K, Dmitrovsky E, Zelent A, Licht JD. 1999. Leukemia translocation protein PLZF inhibits cell growth and expression of cyclin A. *Oncogene* 18:925–934.
- Zakany J, Kmita M, Duboule D. 2004. A dual role for Hox genes in limb anterior-posterior asymmetry. *Science* 304:1669–1672.
- Zuniga A, Zeller R. 1999. Gli3 (Xt) and formin (ld) participate in the positioning of the polarising region and control of posterior limb-bud identity. *Development* 126:13–21.
- Zuniga A, Michos O, Spitz F, Haramis AP, Panman L, Galli A, Vintersten K, Klasen C, Mansfield W, Kuc S, Duboule D, Dono R, Zeller R. 2004. Mouse limb deformity mutations disrupt a global control region within the large regulatory landscape required for Gremlin expression. *Genes Dev* 18:1553–1564.